

# Gravitational waves from coalescing compact binaries\*

Eric Poisson<sup>†</sup>

Department of Physics  
Washington University  
St. Louis, Missouri 63130, USA

## Abstract

This article is intended to provide a pedagogical account of issues related to, and recent work on, gravitational waves from coalescing compact binaries (composed of neutron stars and/or black holes). These waves are the most promising for kilometer-size interferometric detectors such as LIGO and VIRGO. Topics discussed include: interferometric detectors and their noise; coalescing compact binaries and their gravitational waveforms; the technique of matched filtering for signal detection and measurement; waveform calculations in post-Newtonian theory and in the black-hole perturbation approach; and the accuracy of the post-Newtonian expansion.

*Contents:* 1. Introduction. 2. Interferometric detectors. 3. Detector noise. 4. More about detector noise. 5. Coalescing compact binaries. 6. Waveform according to the quadrupole formula. 7. Matched filtering. 8. The signal-to-noise ratio. 9. Signal detection. 10. Signal measurement. 11. Waveform calculations: post-Newtonian theory. 12. Waveform to second post-Newtonian order. 13. Waveform calculations: perturbation theory. 14. Luminosity from the perturbation approach. 15. Accuracy of the post-Newtonian expansion. 16. Conclusion.

## 1 Introduction

The existence of gravitational waves is an unambiguous prediction of the theory of general relativity [1]. Yet, despite efforts originating in the early nineteen sixties, gravitational waves have not been detected directly. Nevertheless, observation of the binary pulsar PSR 1913+16 convinces us that gravitational waves do exist, and that they are correctly described by Einstein's theory [2]. That gravitational waves have not yet been detected on Earth is simply due to their incredible weakness: typical waves would produce in a bulk of matter a strain  $\Delta L/L$ , where  $L$  is the extension of the matter, of order  $10^{-21}$  [1]. Needless to say, to measure this effect is a great challenge for experimentalists.

## 2 Interferometric detectors

There is reasonable hope that gravitational waves will be detected within the next ten years, thanks to a new generation of detectors which use interferometry to monitor the small displacements induced by the passage of a gravitational wave. Two groups are currently involved in building large-scale interferometers: the American LIGO team, and the French-Italian VIRGO team.

The LIGO (Laser Interferometer Gravitational-wave Observatory) project [3] involves two detectors, to be built in Hanford, Washington, and in Livingston, Louisiana. Construction has begun at both sites. Each interferometer has an armlength of approximately 4 km. LIGO should be completed by the turn of the century.

---

\*To appear in the *Proceedings of the Sixth Canadian Conference on General Relativity and Relativistic Astrophysics*.

<sup>†</sup>Address after September 1, 1995: Department of Physics, University of Guelph, Guelph, Ontario, Canada N1G 2W1.

The VIRGO (so named after the galaxy cluster) project [4] involves a single interferometer, to be built near Pisa, Italy, with an armlength of approximately 3 km. VIRGO should also be completed by the turn of the century.

The basic idea behind interferometric detectors is the following [1]:

The interferometer is composed of two long (4 km for LIGO) vacuum pipes forming the letter **L**. A laser beam is split in two at the corner of the **L**, and is sent into each arm of the interferometer. Each beam then bounces off a mass which is suspended at each end of the **L** (a mirror has been coated onto each mass). The light is finally recombined at the beam splitter, and its intensity is measured by a photodiode.

When no gravitational wave is present at the interferometer, the length of each arm is so adjusted that when measured by the photodiode, the light's intensity is precisely zero (the recombined beams are arranged to be precisely out of phase). However, when a gravitational wave passes through the interferometer, the armlengths are no longer constant, and the recombined beams no longer precisely out of phase. More precisely, during the first half of its cycle the gravitational wave increases the length of one arm, and decreases the length of the other. During the second half cycle, the first arm is now shorter, and the second arm longer. The light's intensity therefore oscillates with the gravitational-wave frequency. The intensity is a measure of  $\Delta L/L = h$ , where  $L$  denotes the interferometer armlength, and  $h$  the gravitational-wave field.

### 3 Detector noise

Interferometers are subject to various sources of noise which limit the detector's sensitivity to gravitational waves. The relative importance of each source depends on the frequency at which the interferometer oscillates [3].

At low frequencies ( $f < 10$  Hz) the detector's sensitivity is limited by seismic noise, which is due to the Earth's seismic activity. At frequencies larger than 10 Hz the seismic noise can be eliminated with sophisticated isolation stacks; these fail at low frequencies.

At high frequencies ( $f > 100$  Hz) the detector's sensitivity is limited by photon shot noise, which is due to statistical errors in the counting of photons by the photodiode. This source of noise can be reduced by increasing the laser power, or making use of "light recycling" [3].

At intermediate frequencies ( $f$  between 10 Hz and 100 Hz) the noise is dominated by thermal noise, which is due to spurious motions of thermal origin. For example, the suspended masses are thermally excited and vibrate with their normal-mode frequencies; this evidently affects the recombined laser beam.

Interferometers are therefore broad-band detectors, with good sensitivity in the range [3]

$$10 \text{ Hz} < f < 1 \text{ 000 Hz.} \tag{1}$$

The required sensitivity for full-scale interferometers is approximately  $h_n \sim 10^{-22}$  at peak sensitivity — a tall order. [The subscript  $n$  stands for "noise level"; we will define  $h_n(f)$  precisely below. A plot of  $h_n(f)$ , appropriate for an interferometric detector with "advanced" sensitivity, is given in Fig. 1.] For comparison, we may mention that the Caltech 40 m prototype has already achieved  $h_n \simeq 10^{-19}$  at peak sensitivity ( $f = 450$  Hz). It is not implausible that improved technology and a factor of 100 in armlength will permit to reach the desired goal.

### 4 More about detector noise

The detector noise can be measured when no gravitational wave is present at the interferometer, the typical situation. Then the detector output  $s(t) = \Delta L(t)/L$  is given by noise alone:

$$s(t) = n(t), \tag{2}$$

where  $n(t)$  represents the noise. The noise is a random process [5]: the function  $n(t)$  takes purely random values. Consequently, the noise can only be studied using statistical methods. In the presence of a gravitational wave, Eq. (2) must be replaced by  $s(t) = h(t) + n(t)$ , where  $h(t)$  is the gravitational-wave field.

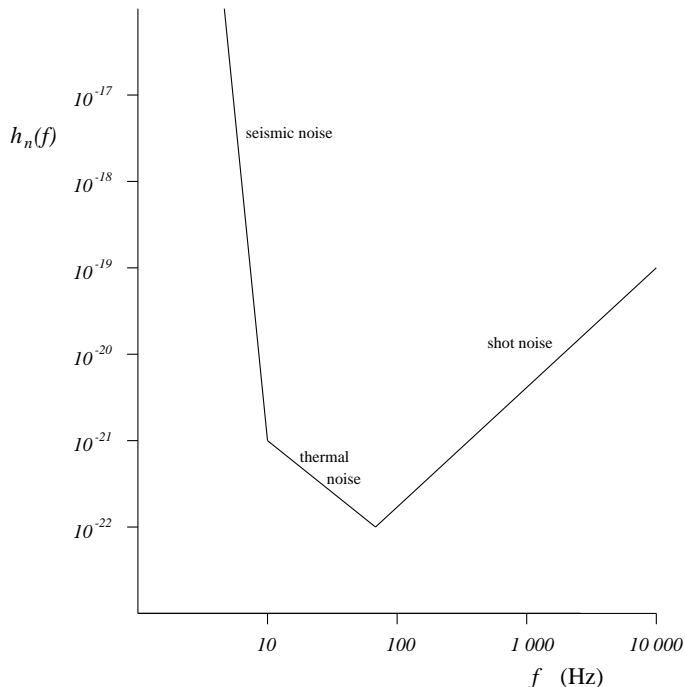


Figure 1: Noise level in an interferometric detector with advanced sensitivity.

The statistical properties of the noise can be determined by careful measurement. For example, the time average

$$\overline{n(t)} = \lim_{T \rightarrow \infty} \frac{1}{2T} \int_{-T}^{+T} n(t) dt \quad (3)$$

can be constructed. This mean value can then be subtracted from  $n(t)$  and, without loss of generality, we can put  $\overline{n} = 0$ . Also from measurements, the noise's *autocorrelation function*  $C_n(\tau)$  can be constructed:

$$C_n(\tau) = \overline{n(t)n(t+\tau)}; \quad (4)$$

$C_n(0)$  gives the mean squared deviation of the noise with respect to the mean value.

In the following we will assume that the noise is *stationary*, in the sense that its statistical properties do not depend on time [5]. This means, in particular, that the autocorrelation function does not depend explicitly on the origin of time  $t$ , but only on the variable  $\tau$ , as was expressed in Eq. (4). We shall also assume that the noise satisfies the *ergodic hypothesis*, so that time averages can be replaced with ensemble averages [5]. Here, the noise is imagined to be drawn from a representative ensemble, and the probability that it takes a particular realization  $n(t)$  is given by a specified probability distribution. The statistical properties of the noise then refer to this (infinite dimensional) distribution function.

In full generality, the statistical properties of the noise can only be summarized by constructing all the higher moments  $\overline{n \cdots n}$ . If, however, the noise is assumed to be Gaussian, in the sense that its probability distribution function is an infinite dimensional Gaussian distribution [6], then the autocorrelation function contains all the information.

Real detector noise is neither strictly stationary nor strictly Gaussian. However, on a timescale of hours, which is long compared with typical gravitational-wave bursts, the noise appears stationary to a good approximation [3]. And non-Gaussian components to the noise can be removed, to a large extent, by cross-correlating detector outputs from two widely separated interferometers [3]. It is therefore a satisfactory approximation to take the noise to be stationary and Gaussian.

Under these assumptions the statistical properties of the detector noise are fully summarized by  $C_n(\tau)$ . It is convenient to work instead in the frequency domain, and to define [5] the noise's *spectral density*  $S_n(f)$

as

$$S_n(f) = 2 \int C_n(\tau) e^{2\pi i f \tau} d\tau. \quad (5)$$

The spectral density is defined for  $f > 0$  only; as  $C_n(\tau)$  is a real and even function, the negative frequencies only duplicate the information contained in the positive frequencies.

As  $n(t)$  is dimensionless, the spectral density has dimensions of time. By multiplying  $S_n(f)$  with the frequency and taking the square root (since the spectral density represents the mean squared noise), one obtains the *noise level*  $h_n(f)$ :

$$h_n(f) = \sqrt{f S_n(f)}. \quad (6)$$

This gives the equivalent gravitational-wave amplitude which would make the interferometer oscillate at just the noise level [1]; this quantity was introduced in the preceding section (see Fig. 1).

## 5 Coalescing compact binaries

Coalescing compact binaries, composed of neutron stars and/or black holes, are the most promising source of gravitational waves for interferometric detectors [1, 7].

Consider the binary pulsar PSR 1913+16 [2]. This system consists of two neutron stars, each of  $1.4 M_\odot$ , in orbital motion around each other. Its present orbital period  $P$  is approximately 8 hours, corresponding to orbital separations of about  $5 \times 10^5$  times the total mass. (Here and throughout we use units such that  $G = c = 1$ .) Its present eccentricity is approximately equal to 0.6.

The binary's orbital period is observed to decay at a rate  $dP/dt = -2 \times 10^{-12}$  corresponding precisely to a loss of energy and angular momentum to gravitational waves [2]. In a timescale of approximately  $10^8$  years the orbital period will have decreased to less than a tenth of a second, corresponding to orbital separations smaller than one hundred times the total mass. In this time, the eccentricity will have been reduced to extremely small values (by the radiation reaction), so that the orbits are practically circular. The gravitational waves produced then have a frequency larger than 10 Hz, and the frequency keeps increasing as the system evolves. *During this late stage of orbital evolution, the gravitational waves sweep through the frequency bandwidth of interferometric detectors, and thus become visible.* By the time the orbital separation becomes as small as a few times the total mass, the neutron stars begin to merge. The gravitational waves produced during the final merger cannot be detected by interferometric detectors, at least in the broad-band configuration described above [8]: the gravitational-wave frequency is then larger than 1 000 Hz, for which the detector noise is large.

Of course, it would be foolish to wait  $10^8$  years in order for PSR 1913+16 to produce gravitational waves with appropriate frequency. Fortunately, interferometric detectors will be sensitive enough to monitor binary coalescences occurring in quite a large volume of the universe, approximately  $10^7$  Mpc<sup>3</sup> (corresponding to a radius of 200 Mpc [3]). It has been estimated [9] that as many as 100 coalescences could occur every year in such a volume (this includes coalescences of black-hole systems as well). This potentially large event rate is one of the factors that make gravitational waves from coalescing compact binaries especially promising.

The other factor comes from the fact that compact binaries are extremely clean astrophysical systems. It can be estimated [10] that tidal interactions between the two stars are completely negligible, up to the point where the objects are about to merge. In particular, no mass transfer occurs. The system can therefore be modeled, to extremely good accuracy, as that of two point masses with a limited number of internal properties (such as mass, spin, and quadrupole moment). The challenge in modeling coalescing compact binaries resides in formulating and solving the equations of motion and wave generation for a general relativistic two-body problem [11].

## 6 Waveform according to the quadrupole formula

At the crudest level, the gravitational-wave signal corresponding to an inspiraling binary system can be calculated by (i) assuming that the orbital motion is Newtonian (with the effects of radiation reaction

incorporated) and (ii) using the standard quadrupole formula for wave generation [12]. As motivated above, we may also assume that the orbits are circular.

We define  $h(t)$  to be the gravitational-wave signal. This is given by a linear combination, appropriate for interferometric detectors, of the two fundamental polarizations,  $h_+$  and  $h_\times$ , of the gravitational-wave field. At this level of approximation, the signal is given by [1]

$$h(t) = Q(\text{angles}) (\mathcal{M}/r) (\pi \mathcal{M} f)^{2/3} \cos \Phi(t). \quad (7)$$

As expected, the signal decays as the inverse power of  $r$ , the distance to the source.

In Eq. (7),  $Q$  is a function of all the angles relevant to the problem: position of the source in the sky, orientation of the orbital plane, position and orientation of the detector on Earth. The parameter  $\mathcal{M}$  is called the *chirp mass* and represents a particular combination of the masses, given by

$$\mathcal{M} = (m_1 m_2)^{3/5} / (m_1 + m_2)^{1/5}. \quad (8)$$

The waveform depends on the chirp mass only, and not on any other combination of the masses. The symbol  $f$  represents the gravitational-wave frequency, which is equal to *twice* the orbital frequency. Because the system loses energy and angular momentum to gravitational waves, the frequency is not constant, but increases in time according to [1]

$$\frac{df}{dt} = \frac{96}{5\pi \mathcal{M}^2} (\pi \mathcal{M} f)^{11/3}. \quad (9)$$

As a consequence, Eq. (7) shows that the amplitude of the signal, which is proportional to  $(\pi \mathcal{M} f)^{2/3}$ , also increases with time. A signal which increases both in frequency and in amplitude is known as a *chirp*, and this is the origin of the term “chirp mass”. Finally, the phase function  $\Phi(t)$  is given by

$$\Phi(t) = \int^t 2\pi f(t') dt'. \quad (10)$$

Because the frequency is not a constant, the phase accumulates nonlinearly with time.

For a system of two neutron stars, the gravitational-wave signal undergoes approximately 16 000 oscillations as it sweeps through the frequency bandwidth of an interferometric detector. The timescale for the frequency sweep is approximately 15 minutes. The orbital separation ranges from approximately 180 to 10 times the total mass  $M = m_1 + m_2$ , and the orbital velocity

$$v \equiv (\pi M f)^{1/3} \quad (11)$$

ranges from approximately 0.1 to 0.4. This indicates that relativistic corrections must be inserted in Eqs. (7) and (9) in order to obtain a satisfactory degree of accuracy.

## 7 Matched filtering

How does one go about finding a gravitational-wave signal in a noisy data stream, when typically the signal is not very strong? And once the signal is found, how does one go about extracting the information it contains? For signals of precisely known form, one goes about this using the technique of *matched filtering* [13]. Signals from inspiraling compact binaries, since they can be calculated with high precision, belong to this class. The basic idea behind matched filtering is to use our knowledge about the signal in order to go find it in the data stream, after the noisy frequencies have been filtered out.

Suppose a signal of known form  $h(t; \vec{\mu})$  is present in the data stream. Here, the vector  $\vec{\mu}$  collectively denotes all the parameters characterizing the signal. In the case of inspiraling binaries, these would be the time of arrival, the initial phase, the distance to the source, the position angles, the chirp mass, and other parameters to be introduced in Sec. 12. The detector output is given by

$$s(t) = h(t; \vec{\mu}) + n(t), \quad (12)$$

where  $n(t)$  is the noise, whose statistical properties are fully summarized by the spectral density  $S_n(f)$ , as discussed in Sec. 4.

The first step in matched filtering [14] is to pass  $s(t)$  through a linear filter which removes the noisy frequencies. The idea here is to use our knowledge about the detector noise contained in  $S_n(f)$  in order to discard that part of the detector output for which the detector noise is large. The output is imagined to be decomposed into Fourier modes according to  $s(t) = \int \tilde{s}(f)e^{-2\pi ift} df$ ; the filter suppresses the modes  $\tilde{s}(f)$  for which  $S_n(f)$  is large.

In mathematical terminology, a linear filter is a linear operation on a function  $s(t)$ . This operation can always be written as [13]

$$s(t) \rightarrow \int w(t-t')s(t') dt', \quad (13)$$

where  $w(t-t')$  is the filter function. The filter which removes the noisy frequencies is the one such that

$$\tilde{w}(f) = \frac{2}{S_n(|f|)}; \quad (14)$$

the factor of 2 is conventional.

The next step in matched filtering consists of computing the overlap integral between the filtered output (13) and the known signal  $h(t; \vec{\mu}_{\text{trial}})$ . The true value  $\vec{\mu}$  of the source parameters is not known prior to the measurement. This operation must therefore be repeated for a large number of trial values  $\vec{\mu}_{\text{trial}}$ ; the corresponding signals  $h(t; \vec{\mu}_{\text{trial}})$  are known as *templates*. The overlap integral defines the function  $S(\vec{\mu}_{\text{trial}})$  given by

$$\begin{aligned} S(\vec{\mu}_{\text{trial}}) &= \int h(t; \vec{\mu}_{\text{trial}})w(t-t')s(t') dt' dt \\ &= \langle h(\vec{\mu}_{\text{trial}}) | s \rangle. \end{aligned} \quad (15)$$

To obtain the second line we have inserted the Fourier decompositions of  $h$ ,  $w$ , and  $s$ , and carried out the integrations over time. The inner product  $\langle \cdot | \cdot \rangle$  is defined as

$$\langle a | b \rangle = 2 \int_0^\infty \frac{\tilde{a}^*(f)\tilde{b}(f) + \tilde{a}(f)\tilde{b}^*(f)}{S_n(f)} df, \quad (16)$$

where  $a$  and  $b$  are arbitrary functions of time, with Fourier transforms  $\tilde{a}$  and  $\tilde{b}$ .

A quantity analogous to  $S(\vec{\mu}_{\text{trial}})$  can be defined for the noise alone, by replacing  $s$  to the right of Eq. (15) by  $n$ . Operationally, this amounts to filtering the detector output when a gravitational-wave signal is known *not* to be present. Because the noise is a random function, the integrals  $\int h(t; \vec{\mu}_{\text{trial}})w(t-t')n(t') dt' dt$  are random also. And because the noise is assumed to have zero mean, to take an average over all possible realizations of the noise (by repeating the measurements many times) would yield a zero value. None of these quantities would be especially useful. We are therefore led to consider the root-mean-square average of these integrals,

$$\begin{aligned} N(\vec{\mu}_{\text{trial}}) &= \text{rms} \int h(t; \vec{\mu}_{\text{trial}})w(t-t')n(t') dt' dt \\ &= \sqrt{\langle h(\vec{\mu}_{\text{trial}}) | h(\vec{\mu}_{\text{trial}}) \rangle} \equiv \rho(\vec{\mu}_{\text{trial}}). \end{aligned} \quad (17)$$

To go from the first to the second line requires some machinery which will not be presented in this review. We refer the reader to Ref. [13] for the missing steps.

## 8 The signal-to-noise ratio

The *signal-to-noise ratio* is defined to be the ratio of  $S$  over  $N$ :

$$\text{SNR}(\vec{\mu}_{\text{trial}}) = \frac{\langle h(\vec{\mu}_{\text{trial}}) | s \rangle}{\rho(\vec{\mu}_{\text{trial}})}. \quad (18)$$

It is clear that  $\text{SNR}(\vec{\mu}_{\text{trial}})$  is a random function, since  $s(t)$  is itself a random function, being the superposition of signal plus noise. Its expectation value, or average over all possible realizations of the noise, is zero in the absence of signal (since  $\bar{n} = 0$ ), and

$$\overline{\text{SNR}(\vec{\mu}_{\text{trial}})} = \frac{\langle h(\vec{\mu}_{\text{trial}}) | h(\vec{\mu}) \rangle}{\rho(\vec{\mu}_{\text{trial}})} \quad (19)$$

in the presence of the signal  $h(t; \vec{\mu})$ . It is important to notice that in Eq. (19), the numerator is the overlap integral between the true signal  $h(t; \vec{\mu})$  and the templates  $h(t; \vec{\mu}_{\text{trial}})$ . In the absence or presence of a signal, the variance in the signal-to-noise ratio is precisely equal to unity [14], independently of the values of  $\vec{\mu}$  and  $\vec{\mu}_{\text{trial}}$ . This fully summarizes the statistical properties of the signal-to-noise ratio, since  $\text{SNR}(\vec{\mu}_{\text{trial}})$  is a Gaussian random function. [This can be seen from the fact that  $s(t)$  itself is Gaussian, being the superposition of signal plus Gaussian noise.]

It is intuitively clear that choosing a template with  $\vec{\mu}_{\text{trial}} = \vec{\mu}$  will produce the largest possible expectation value of the signal-to-noise ratio. This statement, known as *Wiener's theorem* [13], can easily be shown to be true by applying Schwarz's inequality to the right-hand side of Eq. (19). We have

$$\max \left\{ \overline{\text{SNR}(\vec{\mu}_{\text{trial}})} \right\} = \overline{\text{SNR}(\vec{\mu})} = \rho(\vec{\mu}) = \sqrt{\langle h(\vec{\mu}) | h(\vec{\mu}) \rangle}. \quad (20)$$

The fact that the signal-to-noise ratio has a variance of unity indicates that a signal can be concluded to be present only if  $\rho(\vec{\mu})$  is significantly larger than 1. We will come back to this point in the next section.

The true value of the source parameters can therefore be determined by maximizing  $\text{SNR}(\vec{\mu}_{\text{trial}})$  over all possible values of the trial parameters. The fact that the signal-to-noise ratio has a variance of unity implies that this determination can only have a limited degree of accuracy. The statistical errors decrease with increasing  $\rho(\vec{\mu})$ ; since this is proportional to the signal's amplitude, a stronger signal gives better accuracy.

Maximizing the signal-to-noise ratio is essentially equivalent to maximizing the overlap integral

$$\langle h(\vec{\mu}_{\text{trial}}) | h(\vec{\mu}) \rangle.$$

It is easy to see how the choice of the parameters  $\vec{\mu}_{\text{trial}}$  can affect the overlap integral. Consider a toy waveform with three parameters: arrival time, initial phase, and chirp mass. A mismatch in the arrival times clearly reduces the overlap integral: the signal and the template, taken to be functions of time, might have support in entirely different regions of the time axis, leading to a vanishing overlap. Supposing that the arrival times are matched, a mismatch in the initial phases can also reduce the overlap integral: the signal and the template might be out of phase with each other, leading to an oscillating integrand and a vanishingly small overlap. Finally, supposing that both the arrival times and initial phases are matched, a mismatch in the chirp masses would also reduce the overlap integral. This is because the chirp mass governs the rate at which the signal's frequency changes with time; cf. Eq. (9). Signal and template, starting at the same time with the same phase, might thereafter go out of phase, thereby reducing the overlap.

## 9 Signal detection

The first order of business when analysing the output of a gravitational-wave detector is to decide whether or not a signal is present. Here we assume that the signal must be of a specific form, corresponding to a coalescing binary system. In this section we discuss signal detection — how the technique of matched

filtering can be employed to find the signal in the noisy data stream. In the next section we will discuss signal measurement — how matched filtering is used to estimate the value of the source parameters once the signal has been found.

As mentioned in the previous section, a signal can be concluded to be present if the maximum value of the signal-to-noise ratio,  $\text{SNR} \equiv \max\{\text{SNR}(\vec{\mu}_{\text{trial}})\}$ , is significantly larger than unity. In fact, there exists a threshold value  $\text{SNR}^*$  such that a signal is concluded to be present, with a certain confidence level, if  $\text{SNR} > \text{SNR}^*$ . To figure out how large this threshold must be is a standard application of the statistical theory of signal detection [6], which was developed largely for the purpose of detecting radar signals. The theory can easily be taken over to the case gravitational-wave signals [15]. To go into the detail of this theory would be outside the scope of this review. We shall simply state that  $\text{SNR}^*$  is fixed by selecting a small, acceptable value for the probability that a signal would falsely be concluded to be present — the false alarm probability. (This is the Neyman-Pearson criterion [6], which is more precisely formulated in terms of the likelihood ratio, the ratio of the probability that a signal is present to the probability that it is absent.) Once  $\text{SNR}^*$  is fixed, the level of confidence that a signal is indeed present increases with  $\text{SNR} > \text{SNR}^*$ . A typical ballpark value for the threshold is  $\text{SNR}^* = 6$ .

In the preceding paragraph it was assumed that the signal-to-noise ratio  $\text{SNR}$  is computed using template waveforms which are functions of the parameters  $\vec{\mu}$  introduced in Sec. 7. These parameters have direct physical meaning; they include the chirp mass and other meaningful parameters to be introduced in Sec. 12. However, since these parameters are *not* estimated during the detection stage of the data analysis (they are estimated only *after* a signal has been found), there is no particular need to parametrize the templates with  $\vec{\mu}$ . In fact, it may be desirable, in order to minimize the computational effort, to parametrize the signal in a completely different way. The new parameters,  $\vec{\alpha}$ , would then have no particular physical significance. What is required is that the new templates,  $h(t; \vec{\alpha})$ , reproduce the behaviour of the expected gravitational-wave signal. In other words, the templates  $h(t; \vec{\mu})$  and  $h(t; \vec{\alpha})$  should span the same “signal space”, but  $h(t; \vec{\alpha})$  should do so most efficiently. Unlike  $h(t; \vec{\mu})$ ,  $h(t; \vec{\alpha})$  need not be derived from the field equations of general relativity. With these new *detection templates*, the signal-to-noise ratio is defined as

$$\text{SNR} = \max\{\text{SNR}(\vec{\alpha})\}, \quad (21)$$

where  $\text{SNR}(\vec{\alpha})$  is defined as in Eq. (18). As before, a signal is concluded to be present if  $\text{SNR} > \text{SNR}^*$ .

## 10 Signal measurement

Once the detection templates  $h(t; \vec{\alpha})$  have been used to conclude that a signal is present in the data stream, they are replaced with the *measurement templates*  $h(t; \vec{\mu}_{\text{trial}})$  in order to estimate the value of the physical parameters  $\vec{\mu}$ .

The procedure to estimate the source parameters was explained in Sec. 8. As was mentioned, the idea is to maximize over all possible values of the trial parameters the overlap integral

$$\langle h(\vec{\mu}) | h(\vec{\mu}_{\text{trial}}) \rangle.$$

We already have discussed the effect of a mismatch in the value of the parameters. What remains to be discussed is the effect of a mismatch in the functional form of the template with respect to that of the true waveform.

The true waveform is governed by the exact laws of general relativity. The template, on the other hand, is necessarily constructed using an approximation to the exact laws. (That approximations must be made in analytic calculations is obvious; in a numerical treatment the approximation resides in the finite differencing of the field equations.) This, clearly, must have an effect on our strategy for extracting the information contained in the gravitational-wave signal. This can be seen simply from the fact that Wiener’s theorem, as stated in Sec. 8, strictly requires signal and template to have the same functional form; they are allowed to differ only in the value of their parameters.



Suppose that gravitational waves coming from a given source are received without noise, so that the true signal  $h(t; \vec{\mu})$  is measured accurately. Suppose also that the true value  $\vec{\mu}$  of the source parameters is known (God has spoken). Then a computation of the overlap integral with  $\vec{\mu}_{\text{trial}} = \vec{\mu}$  but with an approximate template  $h(t; \vec{\mu}_{\text{trial}})$  will not yield the maximum possible value for  $\text{SNR}(\vec{\mu}_{\text{trial}})$ . This is because the approximation differs from the true signal, both in amplitude and in phase. Since both signal and template undergo a large number of oscillations (recall that for a system of two neutron stars, this number is approximately 16 000), the overlap integral is most sensitive to phase differences: a slight phase lag causes the integrand to oscillate, thereby severely reducing the signal-to-noise ratio with respect to its maximum possible value.

A gravitational-wave astronomer doesn't know before the measurement the true value of the source parameters, and must work with an approximation to the true general-relativistic waveform. We have seen that the phase lag occurring between the true signal and the approximate template when the parameters are matched reduces the signal-to-noise ratio from its maximum possible value. It follows that maximizing  $\text{SNR}(\vec{\mu}_{\text{trial}})$  with approximate templates introduce *systematic errors* into the estimation of the source parameters: evaluating the signal-to-noise ratio with  $\vec{\mu}_{\text{trial}} = \vec{\mu} + \delta\vec{\mu}$  will return, for some  $\delta\vec{\mu}$ , a number larger than  $\text{SNR}(\vec{\mu})$ . The systematic errors are precisely the value of  $\delta\vec{\mu}$  for which the signal-to-noise ratio is largest. If the templates are a poor approximation to the true signal, then the systematic errors will be larger than the statistical errors arising because  $\text{SNR}(\vec{\mu}_{\text{trial}})$  is a random function (see Sec. 8).

We therefore appreciate the need for constructing measurement templates which are as accurate as possible, especially in phase [16, 17]. The requirement is that the systematic errors in the estimated parameters must be smaller than the statistical errors. An estimate for the required degree of accuracy comes from the observation that the overlap integral will be significantly reduced if the template loses phase by as much as one wave cycle with respect to the true signal. Since the total number of wave cycles is approximately 16 000, we have

$$\text{accuracy} \sim \frac{1}{16\,000} \sim 10^{-4}. \quad (22)$$

Since the orbital velocity  $v$  is of order  $10^{-1}$  when the gravitational-wave frequency is in the relevant bandwidth, relativistic corrections *at least* of order  $v^4$  are required to improve the quadrupole-formula expression given in Sec. 6. As we shall see, this is an underestimate.

## 11 Waveform calculations: post-Newtonian theory

We have seen that accurate measurement templates are required to make the most of the gravitational-wave signals originating from coalescing compact binaries. We also have seen that the quadrupole-formula waveform, Eq. (7), is not sufficiently accurate; relativistic corrections at least of order  $v^4$  are required. How does one go about calculating these?

A possible line of approach is to use a slow-motion approximation to the equations of general relativity. This is based on the requirement that if  $v$  is a typical velocity inside the matter source, then

$$v \ll 1. \quad (23)$$

We shall call this approximation “post-Newtonian theory” [18]. We point out that for binary systems, post-Newtonian theory makes no assumption regarding the relative size of the two masses. This is to be contrasted with the perturbation approach, discussed in Sec. 13, in which the mass ratio is assumed to be small, but no restriction is put on  $v$ .

In post-Newtonian theory [19], one starts by defining fields  $h^{\alpha\beta}$  as

$$h^{\alpha\beta} = \sqrt{-g} g^{\alpha\beta} - \eta^{\alpha\beta}, \quad (24)$$

where  $g^{\alpha\beta}$  is the inverse of the true metric  $g_{\alpha\beta}$  with determinant  $g$ , and  $\eta^{\alpha\beta}$  is the metric of Minkowski spacetime. When the harmonic gauge conditions

$$\partial_\beta h^{\alpha\beta} = 0 \quad (25)$$

are imposed, the *exact* Einstein field equations reduce to

$$\square h^{\alpha\beta} = 16\pi(-g)T^{\alpha\beta} + \Lambda^{\alpha\beta}. \quad (26)$$

Here,  $\square = \eta^{\alpha\beta}\partial_\alpha\partial_\beta$  is the flat-spacetime wave operator,  $T^{\alpha\beta}$  is the stress-energy tensor of the source, and  $\Lambda^{\alpha\beta}$  is nonlinear in  $h^{\alpha\beta}$  and represents an effective stress-energy tensor for the gravitational field.

The detailed way in which one solves these equations is quite complicated, and will not be described here. The essential ideas are these [19]:

One first integrates the equations in the near zone ( $r < \lambda$ , where  $r$  is the flat-space radius and  $\lambda$  the gravitational wavelength) assuming slow motion, or  $\partial h^{\alpha\beta}/\partial t \ll \partial h^{\alpha\beta}/\partial x^i$ . One does this by iterations: the nonlinear terms in Eq. (26) are first neglected, and the resulting linear equations integrated. These solutions are then used as input for the next iteration. This process is continued until the desired degree of accuracy is obtained. This is the standard post-Newtonian approach [11].

One next integrates the equations everywhere in the vacuum region outside the source. This is done once again by iterations, assuming  $h^{\alpha\beta} \ll 1$ , but assuming nothing about the relative size of  $\partial h^{\alpha\beta}/\partial t$  with respect to the spatial derivatives. This is because the vacuum region contains the wave zone, in which the field propagates with the speed of light; a slow-motion assumption would therefore not do for the field itself. This is the post-Minkowskian approach [11].

Using the post-Minkowskian approach one constructs, by successive approximations, the most general solution to the Einstein equations outside the source. This is characterized by two infinite sets of arbitrary multipole moments [20], the mass moments  $M_{\ell m}(t-r)$  and the current moments  $J_{\ell m}(t-r)$ , where  $\ell$  and  $m$  are the standard spherical-harmonic indices. (In practice, the fields  $h^{\alpha\beta}$  are equivalently expressed in terms of symmetric-trace-free moments, not spherical-harmonic moments.) The general solution is then matched to the near-zone solution in the region of common validity, and the multipole moments are thus determined.

Finally, one expresses the radiation field — the time-varying,  $O(1/r)$  part of the gravitational field — in terms of the derivatives of the mass and current multipole moments [20]. This gives the gravitational waveform. The gravitational-wave luminosity  $dE/dt$  can also be obtained from the radiation field.

## 12 Waveform to second post-Newtonian order

To date, the post-Newtonian calculation of the waveform has been carried out accurately through second post-Newtonian order —  $O(v^4)$  — beyond the leading-order, quadrupole-formula expressions given in Sec. 6. The complete waveform will not be displayed here. Instead, we will focus solely on the waveform’s *phasing*.

The phasing of the waves can be determined from  $df/dt$ , the rate of change of the gravitational-wave frequency. This can be expressed as

$$\frac{df}{dt} = \frac{dE/dt}{dE/df}, \quad (27)$$

where  $dE/dt$  is (minus) the gravitational-wave luminosity, and  $dE/df$  relates orbital energy to orbital frequency ( $f$  is twice the orbital frequency; the orbits are assumed to be circular). Both these quantities can be expanded in powers of

$$v \equiv (\pi Mf)^{1/3}, \quad (28)$$

with leading-order terms [12]

$$\left(\frac{dE}{dt}\right)_N = -\frac{32}{5}\eta^2 v^{10}, \quad \left(\frac{dE}{df}\right)_N = -\frac{\pi}{3}\mu M v^{-1}, \quad (29)$$

where the subscript  $N$  stands for “Newtonian”. We have introduced the reduced mass  $\mu$ , the total mass  $M$ , and the mass ratio  $\eta$  as

$$\mu = \frac{m_1 m_2}{m_1 + m_2}, \quad M = m_1 + m_2, \quad \eta = \frac{\mu}{M}. \quad (30)$$

Notice that  $\eta$  is restricted to the interval  $0 < \eta \leq 1/4$ , with  $\eta = 1/4$  for  $m_1 = m_2$ . It is easy to check that Eqs. (27) and (29) reproduce Eq. (9) above; the chirp mass can be expressed as  $\mathcal{M} = \eta^{3/5} M$ .

For simplicity we will, in the following, focus on the quantity  $dE/dt$ . To second post-Newtonian order, the luminosity takes the form

$$\frac{dE}{dt} = \left( \frac{dE}{dt} \right)_N \left[ 1 - \left( \frac{1247}{336} + \frac{35}{12} \eta \right) v^2 + (4\pi - \text{SO}) v^3 - \left( \frac{44711}{9072} - \frac{9271}{504} \eta - \frac{65}{18} \eta^2 + \text{SS} \right) v^4 + \dots \right]. \quad (31)$$

Here, the terms SO and SS are due to spin-orbit and spin-spin interactions, respectively [21]; these occur if the masses  $m_1$  and  $m_2$  are rotating. Let  $\vec{S}_1$  and  $\vec{S}_2$  be the spin angular momentum of each mass, and define the dimensionless quantities  $\vec{\chi}_a = \vec{S}_a/m_a^2$ , for  $a = \{1, 2\}$ . Let also  $\hat{L}$  be the direction of orbital angular momentum. Then [21]

$$\text{SO} = \frac{1}{4} \sum_{a=1}^2 \left[ 11(m_a/M)^2 + 5\eta \right] \hat{L} \cdot \vec{\chi}_a \quad (32)$$

is the spin-orbit term, and

$$\text{SS} = \frac{\eta}{48} \left( 103 \vec{\chi}_1 \cdot \vec{\chi}_2 - 289 \hat{L} \cdot \vec{\chi}_1 \hat{L} \cdot \vec{\chi}_2 \right) \quad (33)$$

is the spin-spin term.

In Eq. (31), the leading-order term was first calculated in 1963 by Peters and Mathews [22] using the standard quadrupole formula. The first post-Newtonian correction, at order  $v^2$ , was calculated in 1976 by Wagoner and Will [23]. The  $4\pi v^3$  term is due to wave propagation effects: As the waves propagate out of the near zone they are scattered by the curvature of spacetime, and this modifies both the amplitude and the phase of the waveform; this “tail term” was first calculated in 1993 by this author [24], and then independently by Wiseman [25] and Blanchet and Schäfer [26]. The second post-Newtonian correction, at order  $v^4$ , was calculated in 1994 by Blanchet, Damour, Iyer, Will, and Wiseman [27]. Finally, the spin-orbit and spin-spin corrections were calculated in 1993 by Kidder, Will, and Wiseman [21].

We see from Eq. (31) that the post-Newtonian corrections bring a number of additional source parameters into the picture. The waveform no longer depends uniquely upon the chirp mass  $\mathcal{M}$ ; it now depends upon the masses  $m_1$  and  $m_2$  separately, and upon the spin-orbit and spin-spin parameters (which stay approximately constant as the system evolves toward coalescence). These new parameters must be included into  $\vec{\mu}$  when the signal is analyzed using matched filtering.

What we have at this point is an expression for the waveform which is accurate to second post-Newtonian order. The question facing us is whether this waveform is sufficiently accurate to be used as measurement templates. In other words, are the systematic errors generated by these templates guaranteed to be smaller than the statistical errors?

Evidently, to answer this question is difficult, since we do not have access to the exact waveform in order to make comparisons. In the next section we will consider a model problem for which the waveform *can* be calculated exactly, thereby enabling us to judge the accuracy of the post-Newtonian expansion. We will find, in Sec. 15, that the answer to this question is, most likely, no: the second post-Newtonian waveform is not sufficiently accurate.

## 13 Waveform calculations: perturbation theory

A different line of attack for solving Einstein’s equations for a compact binary system is to assume that one of the bodies is very much less massive than the other [28]. We therefore demand

$$\mu/M \ll 1, \quad (34)$$

where  $\mu$  is the reduced mass and  $M$  the total mass. In this limit  $\mu$  is practically equal to the smaller mass  $m_1$ , and  $M$  is practically equal to the larger mass  $m_2$ . In contrast with the post-Newtonian approach, we assume *nothing* about the size of the velocity  $v$ .

This approach takes advantage of the fact that when Eq. (34) is valid, the smaller mass creates only a small perturbation in the gravitational field of the larger mass, which can be taken to be the Schwarzschild field. The total gravitational field can therefore be written as

$$g_{\alpha\beta} = g_{\alpha\beta}^{(0)} + h_{\alpha\beta}, \quad (35)$$

where  $g_{\alpha\beta}^{(0)}$  represents the background Schwarzschild metric, and  $h_{\alpha\beta}$  the perturbation.

Writing Einstein's equations for  $g_{\alpha\beta}$  and linearizing with respect to  $h_{\alpha\beta}$ , one finds that the perturbation must satisfy an inhomogeneous wave equation in the Schwarzschild spacetime. Schematically,

$$\square^{\alpha\beta\mu\nu} h_{\mu\nu} = 8\pi T^{\alpha\beta}, \quad (36)$$

where  $\square^{\alpha\beta\mu\nu}$  is an appropriate curved-spacetime wave operator, and  $T^{\alpha\beta}$  the stress-energy tensor associated with the orbiting mass.

We will specifically assume that the central body is a Schwarzschild black hole of mass  $M$ . This assumption is made for simplicity, and removes the need to model the star's interior. As a matter of fact, the internal structure of the bodies is irrelevant, except during the last few orbital cycles before coalescence; this was discussed in Sec. 5. Taking advantage of this, we model the orbiting body as a point particle of mass  $\mu$ , so that its stress-energy tensor is a Dirac distribution with support on the particle's world line. For simplicity, and also because it is physically well motivated (as explained in Sec. 5), we take the world line to be a circular geodesic of the Schwarzschild spacetime. With  $\{t, r, \theta, \phi\}$  as the usual Schwarzschild coordinates,  $r_0$  denotes the orbital radius, and  $\Omega = d\phi/dt$  is the angular velocity. We have

$$v \equiv \Omega r_0 = (M/r_0)^{1/2} = (M\Omega)^{1/3}, \quad (37)$$

and the gravitational-wave frequency  $f$  is given by  $2\pi f = 2\Omega$ . We stress once more that in the perturbation approach,  $v$  is not required to be small. The only limitation on  $v$  comes from the fact that for  $r_0 \leq 6M$ , circular orbits are no longer stable; this implies  $v < 6^{-1/2} \simeq 0.4082$ .

Black-hole perturbations are conveniently treated with the Teukolsky formalism [29], in which gravitational perturbations are represented by the complex-valued function  $\Psi_4$ , a particular component of the perturbed Weyl tensor; the tensor  $h_{\alpha\beta}$  can be reconstructed from  $\Psi_4$ . The equation satisfied by  $\Psi_4$  admits a separation of the variables. When  $\Psi_4$  is expanded in spherical harmonics and decomposed into Fourier modes  $e^{-i\omega t}$ , one obtains an ordinary second-order differential equation — the Teukolsky equation — for the radial function  $R_{\omega\ell m}(r)$ . Here,  $\ell$  and  $m$  are the usual spherical-harmonic indices. Schematically, and omitting the subscript  $\omega\ell m$ , this equation takes the form

$$\mathcal{D}R(r) = T(r), \quad (38)$$

where  $\mathcal{D}$  is a second-order differential operator, and  $T(r)$  the source, constructed from the particle's stress-energy tensor [28].

Equation (38) can be integrated in the standard way by constructing a Green's function  $G(r, r')$  out of two linearly independent solutions to the homogeneous equation. These solutions,  $R_{<}(r)$  and  $R_{>}(r)$ , respectively satisfy appropriate boundary conditions at the inner ( $r = 2M$ ) and outer ( $r = \infty$ ) boundaries. Schematically,  $G(r, r') = R_{<}(r_{<})R_{>}(r_{>})$ , where  $r_{<}$  ( $r_{>}$ ) is the lesser (greater) of  $r$  and  $r'$ . The solution to Eq. (38) can then be expressed as  $R(r) = \int G(r, r')T(r') dr'$ , and  $\Psi_4$  can be reconstructed by summing over all the modes. Finally, the gravitational waveform  $h$  and the luminosity  $dE/dt$  can be obtained from the asymptotic behaviour of  $\Psi_4$  when  $r \rightarrow \infty$ .

To integrate Eq. (38) therefore reduces to solving the homogeneous Teukolsky equation,  $\mathcal{D}R(r) = 0$ , for the functions  $R_{<}(r)$  and  $R_{>}(r)$ . This, it turns out, is equivalent to integrating the Regge-Wheeler equation [30]

$$\left\{ \frac{d^2}{dr^{*2}} + \omega^2 - \left( 1 - \frac{2M}{r} \right) \left[ \frac{\ell(\ell+1)}{r^2} - \frac{6M}{r} \right] \right\} X_{\omega\ell}(r) = 0, \quad (39)$$

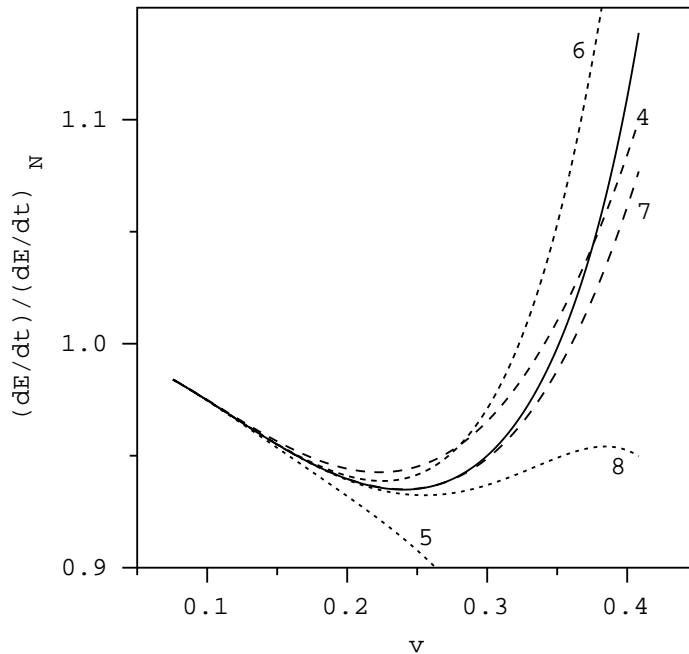


Figure 2: Various representations of  $(dE/dt)/(dE/dt)_N$  as a function of orbital velocity  $v$ . The solid curve represents the exact results, obtained numerically. The various broken curves represent the various post-Newtonian approximations, as explained in the text.

for the functions  $X_<(r)$  and  $X_>(r)$ ; here,  $d/dr^* = (1 - 2M/r)d/dr$ . This comes about because a solution to the homogeneous Teukolsky equation can easily be related to a solution to the Regge-Wheeler equation. The relation is known as the Chandrasekhar transformation [31].

## 14 Luminosity from the perturbation approach

The problem of calculating the gravitational waveform for a compact binary system with small mass ratio can therefore be reduced to the simple one of integrating Eq. (39). The relevant dimensionless parameter entering this equation is  $M\omega$ , where, for circular orbits,  $\omega = m\Omega$  [28]. We therefore have, using Eq. (37),  $M\omega = mv^3$ .

For arbitrary values of  $M\omega$  the Regge-Wheeler equation must be integrated numerically [32]. This must be done separately for each selected value of  $v$  in the interval  $0.1 < v < 0.4$  (approximately corresponding, for systems of a few solar masses, to the frequency interval  $10 \text{ Hz} < f < 1000 \text{ Hz}$ ). [5]

Once again we will focus on  $dE/dt$ , the gravitational-wave luminosity. In Fig. 2 we present a plot of  $(dE/dt)/(dE/dt)_N$  as a function of  $v$ . This is the ratio of the luminosity as calculated exactly (numerically) using the perturbation approach, to the quadrupole-formula expression

$$\left(\frac{dE}{dt}\right)_N = -\frac{32}{5}\left(\frac{\mu}{M}\right)^2 v^{10}. \quad (40)$$

The numerical results are depicted as a solid curve. Apart from negligible numerical errors, these results are *exact* to all orders in  $v$ ; the only assumption used in the calculation concerns the smallness of  $\mu/M$ . The various broken curves will be described below. The figure shows that  $(dE/dt)/(dE/dt)_N$  tends toward unity as  $v \rightarrow 0$ , and stays within 15% of unity everywhere in the interval  $0 < v < 6^{-1/2}$ .

It is now easy to judge the accuracy of the post-Newtonian expansion for  $dE/dt$  in the limit  $\mu/M \rightarrow 0$ . One simply evaluates Eq. (31) in this limit, with  $\text{SO} = \text{SS} = 0$ , and compare with the numerical results. This

post-Newtonian curve is labeled “4” in the figure, and we see that the numerical results are only imperfectly reproduced. The consequences of this will be discussed in the next section.

One can in fact do better than this. The perturbation approach is not only suitable for exact, numerical computations. By combining it with a slow-motion approximation — putting  $v \ll 1$  on top of  $\mu/M \ll 1$  — it also becomes suitable for approximate, analytical computations. Methods for integrating the Regge-Wheeler equations analytically in the limit  $M\omega \ll 1$  were devised by various authors [24, 28, 33]. The basic idea is to proceed by iterations: Eq. (39) with  $M\omega = 0$  is solved in terms of spherical Bessel functions, and this zeroth order solution is used as input for the first iteration.

Using these methods, Tagoshi and Sasaki [34] were able to calculate  $dE/dt$  analytically, accurately through fourth post-Newtonian order, two full orders beyond Eq. (31). They derive the rather impressive expression

$$\begin{aligned} \frac{dE}{dt} = & \left( \frac{dE}{dt} \right)_N \left[ 1 - \frac{1247}{336} v^2 + 4\pi v^3 - \frac{44711}{9072} v^4 - \frac{8191}{672} \pi v^5 \right. \\ & + \left( \frac{6643739519}{69854400} - \frac{1712}{105} \gamma + \frac{16}{3} \pi^2 - \frac{3424}{105} \ln 2 - \frac{1712}{105} \ln v \right) v^6 - \frac{16285}{504} \pi v^7 \\ & + \left( -\frac{323105549467}{3178375200} + \frac{232597}{4410} \gamma - \frac{1369}{126} \pi^2 + \frac{39931}{294} \ln 2 - \frac{47385}{1568} \ln 3 + \frac{232597}{4410} \ln v \right) v^8 \\ & \left. + \dots \right]. \end{aligned} \quad (41)$$

Notice the presence of  $\ln v$  terms in this expansion, as well as that of the Euler number  $\gamma \simeq 0.5772$ . Notice also that the first four terms reproduce Eq. (31) in the limit  $\mu/M \rightarrow 0$ , when  $\text{SO} = \text{SS} = 0$ . This, of course, is as it should be.

The broken curves in Fig. 2 represent plots of Eq. (41) truncated to various orders in  $v$ . For example, the curve labeled “6” is a plot of Eq. (41) with all terms of order  $v^7$  and  $v^8$  discarded. We see from the figure that the post-Newtonian expansion converges poorly. (The suspicion, in fact, is that the series is only asymptotic.) Witness in particular the poor quality of the curve “5” with respect to “4”, and compare also “8” to “7”.

## 15 Accuracy of the post-Newtonian expansion

We have seen that in the  $\mu/M \rightarrow 0$  limit, the post-Newtonian expansion for  $dE/dt$  converges poorly. A similar statement can be made about  $dE/df$ : the post-Newtonian expansion

$$\frac{dE}{df} = \left( \frac{dE}{df} \right)_N \left( 1 - \frac{3}{2} v^2 - \frac{81}{8} v^4 - \frac{675}{16} v^6 - \frac{19845}{128} v^8 + \dots \right), \quad (42)$$

where

$$\left( \frac{dE}{df} \right)_N = -\frac{\pi}{3} \mu M v^{-1}, \quad (43)$$

converges slowly to the exact result [35]

$$\frac{dE}{df} = \left( \frac{dE}{df} \right)_N (1 - 6v^2)(1 - 3v^2)^{-3/2}. \quad (44)$$

Contrary to Eq. (41), the expansion (42) is actually *known* to converge (for all values of  $v$  in the interval  $0 < v < 6^{-1/2}$ ).

In this section we address the issue as to how much of an obstacle the poor convergence of the post-Newtonian expansion poses to the construction of accurate measurement templates [36]. We will answer this question for binary systems with small mass ratios, using the results described in the preceding section.

$n$	PN	EXACT
4	0.5796	0.4958
5	0.4646	0.5286
6	0.7553	0.9454
7	0.7651	0.9864
8	0.7568	0.9695

Table 1: Reduction in signal-to-noise ratio incurred when matched filtering with approximate, post-Newtonian templates. The first column lists the order  $n$  of the approximation, the second column lists  $\mathcal{R}_n$  as calculated using the post-Newtonian approximation for  $dE/df$ , and the third column lists  $\mathcal{R}_n$  as calculated using the exact expression for  $dE/df$ .

Since there is no reason to believe that the convergence of the post-Newtonian expansion would be much improved for systems of comparable masses, our results should also apply, at least qualitatively, for such systems.

One way to address this question is to ask, given a waveform constructed from the exact numerical results, how much signal-to-noise ratio is lost by matched filtering the exact signal with an approximate post-Newtonian template?

From Sec. 8 we know that filtering with the exact signal  $h(t)$  would give  $\text{SNR}|_{\text{max}}$ , the largest possible value of the signal-to-noise ratio. On the other hand, filtering with a post-Newtonian template  $h_n$ , where  $n$  denotes the order in  $v$  to which the expansion is taken (for example,  $n = 4$  represents a waveform accurate to second post-Newtonian order), gives the smaller value  $\text{SNR}|_{\text{actual}}$ . From the results of Sec. 7 and 8 we obtain

$$\mathcal{R}_n \equiv \frac{\text{SNR}|_{\text{actual}}}{\text{SNR}|_{\text{max}}} = \frac{|\langle h|h_n \rangle|}{\sqrt{\langle h|h \rangle \langle h_n|h_n \rangle}}. \quad (45)$$

The detail of how to compute  $\mathcal{R}_n$  is presented in Ref. [36].

The calculation described here can only be carried out for binary systems with small mass ratios, because only for these do we have access to the exact waveform  $h(t)$ . Nevertheless, in the following we shall let  $\mu/M$  become large, without altering our expressions for the exact and post-Newtonian waveforms. This is done without justification, but reflects the adopted point of view that the quality of the post-Newtonian approximation should not be appreciably affected by the finite-mass corrections.

In doing this extrapolation, some thought must be given as to the interpretation of the ratio  $\mu/M$ . In the limit  $\mu/M \rightarrow 0$  this can be taken to be both the ratio of the individual masses or the ratio of reduced mass to total mass. In the case of comparable masses, some choice must be made. We note that as  $\mu/M$  is allowed to grow large, expressions (40) and (43) for the Newtonian quantities  $(dE/dt)_N$  and  $(dE/df)_N$  must be replaced by expressions (29), *which are formally identical*. This shows that when extrapolating to the case of comparable masses,  $\mu$  is to be interpreted as the *reduced mass*, and  $M$  as the *total mass*.

We quote the results for  $\mathcal{R}_n$  corresponding to a system of two neutron stars, each of  $1.4 M_\odot$ ; these are displayed in the second column of Table 1. We see that even at quite a high order in the post-Newtonian expansion, only three quarters of the signal-to-noise ratio is reproduced by the post-Newtonian template. This shows that the apparently small discrepancies between the exact and post-Newtonian results for  $dE/dt$  and  $dE/df$  provide a serious obstacle to the construction of accurate measurement templates.

It is interesting to ask how much of the signal-to-noise ratio would be recovered if  $dE/df$  were kept exact instead of being expressed as a post-Newtonian expansion. The third column of the table displays the values of  $\mathcal{R}_n$  calculated in this way. We see that most of the signal-to-noise is recovered:  $\mathcal{R}_n$  can now be as large as 0.9864 instead of 0.7651. Why does the exact expression for  $dE/df$  give such better results? It can be established [36] that this has to do with the following fact: While the exact expression for  $dE/df$  correctly goes to zero at  $v = 6^{-1/2}$  (at the innermost circular orbit), its post-Newtonian analogue fails to do so.

[For example, the right-hand side of Eq. (42), truncated to order  $v^8$ , goes to zero at  $v \simeq 0.4236 > 6^{-1/2}$ , corresponding to a radius  $r_0 \simeq 5.572M$ .] When corrected for this, the post-Newtonian template gives much better results.

## 16 Conclusion

We therefore see that the poor convergence of the post-Newtonian expansion is a serious obstacle to the construction of accurate measurement templates. Devising ways to extract the information contained in gravitational waves produced during the late inspiral of a compact binary system poses a great challenge to theoretical physicists. It is not clear that “simply” pushing to higher order in post-Newtonian theory will be enough to produce sufficiently accurate measurement templates (such that the systematic errors will be smaller than the statistical errors). There may be a need for theorists to develop alternative ways of dealing with this problem.

It should be stressed that the convergence problem does not arise when constructing *detection templates*. Indeed, as was discussed in Sec. 9, there is no particular need for these templates to be derived from the equations of general relativity. And since the detection templates need not involve any parameters of direct physical significance, the notion of systematic errors does not apply to them. The only requirement for constructing detection templates is that they should span the appropriate “signal space”, and that they should do so the most efficiently.

The poor convergence of the post-Newtonian expansion is therefore not an obstacle for *detecting* gravitational waves from coalescing compact binaries. It is only an obstacle for extracting the information that the waves contain. To overcome this obstacle will undoubtedly be a theorist’s challenge for years to come. This state of affairs is highly interesting from a historical point of view: Never before in the history of gravitational physics has experiment demanded such a high degree of sophistication on theoretical calculations.

## Acknowledgments

This work was supported by the Natural Sciences Foundation under Grant No. PHY 92-22902 and the National Aeronautics and Space Administration under Grant No. NAGW 3874. This article was completed while visiting the Theoretical Physics Institute of the University of Alberta; the author is most grateful to Werner Israel for his warm hospitality.

## References

- [1] For broader reviews on gravitational waves, see K.S. Thorne, in *300 Years of Gravitation*, edited by S.W. Hawking and W. Israel (Cambridge University Press, Cambridge, 1987); in *Proceedings of the Snowmass 95 Summer Study on Particle and Nuclear Astrophysics and Cosmology*, edited by E.W. Kolb and R. Peccei (World Scientific, Singapore, 1995).
- [2] R.A. Hulse and J.H. Taylor, *Astrophys. J.* **324**, 355 (1975); J.H. Taylor, *Rev. Mod. Phys.* **66**, 711 (1994).
- [3] A. Abramovici *et al.*, *Science* **256**, 325 (1992).
- [4] C. Bradaschia *et al.*, *Nucl. Instrum. & Methods* **A289**, 518 (1990).
- [5] See, for example, F. Reif, *Fundamentals of Statistical and Thermal Physics* (McGraw-Hill, New-York, 1965).
- [6] C.W. Helstrom, *Statistical Theory of Signal Detection* (Pergamon, Oxford, 1968).
- [7] B.F. Schutz, *Nature (London)* **323**, 310 (1986); *Class. Quantum Grav.* **6**, 1761 (1989).



- [8] Other configurations, with narrow-band sensitivity at a chosen frequency, are possible.
- [9] E.S. Phinney, *Astrophys. J.* **380**, L17 (1991); R. Narayan, T. Piran, and A. Shemi, *ibid.* **379**, L17 (1991); A.V. Tutukov and L.R. Yungelson, *Mon. Not. Roy. Astron. Soc.* **260**, 675 (1993).
- [10] C. Kochanek, *Astrophys. J.* **398**, 234 (1992); L. Bildsten and C. Cutler, *ibid.* **400**, 175 (1992).
- [11] For an overview, see T. Damour, in *300 Years of Gravitation*, edited by S.W. Hawking and W. Israel (Cambridge University Press, Cambridge, 1987).
- [12] See, for example, C.W. Misner, K.S. Thorne, and J.A. Wheeler, *Gravitation* (Freeman, San Francisco, 1973), Chap. 36.
- [13] L.A. Wainstein and V.D. Zubakov, *Extraction of Signals from Noise* (Prentice-Hall, Englewood Cliffs, 1962).
- [14] The following discussion is based on C. Cutler and E.E. Flanagan, *Phys. Rev. D* **49**, 2658 (1994).
- [15] L.S. Finn, *Phys. Rev. D* **46**, 5236 (1992).
- [16] L.S. Finn and D.F. Chernoff, *Phys. Rev. D* **47**, 2198 (1993).
- [17] C. Cutler *et al.*, *Phys. Rev. Lett.* **70**, 1984 (1993).
- [18] For an overview, see C.M. Will, in *Relativistic Cosmology*, Proceedings of the Eighth Nishinomiya-Yukawa Memorial Symposium, edited by M. Sasaki (Universal Academy Press, Kyoto, 1994).
- [19] The following discussion is based on the work of Blanchet, Damour, and Iyer, expounded in the following papers: L. Blanchet and T. Damour, *Philos. Trans. R. Soc. London A* **320**, 379 (1986); *Phys. Rev. D* **37**, 1410 (1988); *Ann. Inst. H. Poincaré (Phys. Théorique)* **50**, 377 (1989); L. Blanchet, *Proc. R. Soc. London A* **409**, 383 (1987); T. Damour and B.R. Iyer, *Ann. Inst. H. Poincaré (Phys. Théorique)* **54**, 115 (1991).
- [20] K.S. Thorne, *Rev. Mod. Phys.* **52**, 299 (1980).
- [21] L.E. Kidder, C.M. Will, and A.G. Wiseman, *Phys. Rev. D* **47**, R4183 (1993).
- [22] P.C. Peters and J. Mathews, *Phys. Rev.* **131**, 435 (1963).
- [23] R.V. Wagoner and C.M. Will, *Astrophys. J.* **210**, 764 (1976); **215**, 984 (1977).
- [24] E. Poisson, *Phys. Rev. D* **47**, 1497 (1993).
- [25] A.G. Wiseman, *Phys. Rev. D* **48**, 4757 (1993).
- [26] L. Blanchet and G. Schäfer, *Class. Quantum Grav.* **10**, 2699 (1993).
- [27] L. Blanchet, T. Damour, B.R. Iyer, C.M. Will, and A.G. Wiseman, *Phys. Rev. Lett.* **74**, 3515 (1995).
- [28] The following discussion is based on the work of this author and his collaborators. See E. Poisson and M. Sasaki, *Phys. Rev. D* **51**, 5753 (1995) and references therein.
- [29] S.A. Teukolsky, *Astrophys. J.* **185**, 635 (1973).
- [30] T. Regge and J.A. Wheeler, *Phys. Rev.* **108**, 1063 (1957).
- [31] S. Chandrasekhar, *Proc. R. Soc. London A* **343**, 289 (1975).
- [32] C. Cutler, L.S. Finn, E. Poisson, and G.J. Sussman, *Phys. Rev. D* **47**, 1511 (1993).

- [33] M. Sasaki, Prog. Theor. Phys. **92**, 17 (1994).
- [34] H. Tagoshi and M. Sasaki, Prog. Theor. Phys. **92**, 745 (1994).
- [35] This can be derived simply from the equations for circular geodesic motion in Schwarzschild.
- [36] E. Poisson, *Gravitational radiation from a particle in circular orbit around a black hole. VI. Accuracy of the post-Newtonian expansion*, Phys. Rev. D, in press.